Discovery-based Protein Expression Profiling Identifies Distinct Subgroups and Pathways in Leiomyosarcomas

Ufuk Kirik[1], Karin Hansson[1], Morten Krogh[2], Mats Jönsson[2], Mef Nilbert[3,4], Peter James[1], Ana Carneiro[3*]*

[1] Department of Immunotechnology, Lund University, Medicon Village, Lund, Sweden
[2] Amber Biosciences AB, Lund, Sweden
[3] Institute of Clinical Sciences, Department of Oncology, Lund University, Sweden
[4] Clinical Research Centre, Hvidovre Hospital, Copenhagen University, Denmark

*Address for correspondence regarding clinical questions should be addressed to AC and technical mass spectrometry questions to PJ.

Conflicts of Interest

No conflict of interest is declared.

RUNNING TITLE: Protein profiling of leiomyosarcoma

ABSTRACT:

Soft tissue sarcomas (STS) are malignant tumors of mesenchymal origin. A substantial portion of these tumors exhibits complex karyotypes and lack characterized chromosomal aberrations. Owing to such properties, both histopathological and molecular classification of these tumors has been a significant challenge. This study examines the protein expression of a large number of human soft-tissue sarcomas, including subtype heterogeneity, using 2D-gel proteomics. In addition, detailed proteome profiles of a subset of pleomorphic STS specimens using an in-depth mass-spectrometry approach and identified subgroups within the leiomyosarcomas with distinct protein expression patterns. Pathways analysis indicates that key biological nodes like apoptosis, cytoskeleton remodeling and telomere regulation are differentially regulated among these subgroups. Finally, investigating the

similarities between protein expression of leiomyosarcomas and undifferentiated pleomorphic sarcomas (UPS) revealed similar protein expression profiles for these tumors, in comparison to pleomorphic leiomyosarcomas.

Implications: These results suggest that UPS tumors share a similar lineage as leiomyosarcomas, and are likely to originate from different stages of differentiation from mesenchymal stem cells to smooth muscle cells.

ABBREVIATIONS:

STS – soft tissue sarcoma

LMS – leiomyosarcoma

MFH – myoxid fibrous histosarcoma

NOS – not otherwise specified

UPS – undifferentiated pleomorphic sarcoma

MS – mass spectrometry

MS/MS – tandem mass spectrometry

TMT – tandem mass tags

ECM – extracellular matrix

FA – focal adhesion

PCA- principal component analysis

Introduction

Soft tissue sarcomas (STS) are rare tumors of mesenchymal origin that are highly malignant and heterogeneous. Metastases develop in approximately one third of the patients, most of whom die from the disease (2). Morphologically more than 50 entities have been described. Based on genetic alterations, STS are broadly divided into tumors with specific reciprocal translocations and simple karyotypes, and tumors with complex karyotypes in which specific aberrations have not been recognized (1,3).

Poorly differentiated sarcomas represent a diagnostic challenge as these tumours lack a typical and easily identifiable phenotype. The undifferentiated diagnostic category is usually considered in four broad groups: tumours with round cell morphology, spindle cell morphology, epithelioid morphology and pleomorphic morphology. The latter group can be simplistically defined as one in which the cells display marked atypia, and should not be taken as synonymous of undifferentiation or biologic aggressiveness. Pleomorphic sarcomas broadly encompass six histotypes (differential diagnoses): pleomorphic liposarcoma, pleomorphic leiomyosarcoma, pleomorphic rhabdomyosarcoma, dedifferentiated liposarcoma, myxofibrosarcoma and malignant fibrous histiocytoma/undifferentiated pleomorphic sarcoma (MFH/UPS). In most cases, with adequate sampling and complementary diagnostic techniques e.g. immunohistochemistry or electron microscopy, a diagnosis is possible, in spite of only focal evidence of a line of differentiation. However, in 5-10% of the cases, no line of differentiation can be identified and these tumours are classified as MFH/UPS, which nowadays essentially represents a diagnosis of exclusion. Until the 1990's, MFH represented the most frequent STS diagnosis, accounting for 40% of all adult mesenchymal malignancies. Despite the heterogeneity of these tumors there are no alternative courses of treatment for different types of STS used at Lund University Hospital, currently.

Genomic profiling studies by comparative genome hybridization and gene expression analyses have increased our insight into the biology of pleomorphic STS (4-11). Similarities in genomic and gene expression profiles suggest that, in the context of STS of the extremities, tumors that are histo-pathologically classified as MFH/UPS may based on genetic alterations corresponding to highly

pleomorphic leiomyosarcomas (LMS) (6,9). Our group has previously performed gene expression analysis on pleomorphic STS, encompassing a series of 40 LMS. Among the LMS, a subgroup of 11 samples clustered together while the remaining 29 LMS showed more heterogeneous patterns of gene expression. The 11-sample cluster showed a high expression of muscle-associated genes. Similar results were reported by van Rijn et al., when analyzing a set of LMS, which could be divided in three subgroups depending on gene expression analysis. The heterogeneity of LMS, morphologically as well as genetically, indicates that further investigations are needed in order to define subtypes and define molecular classifiers.

Data on the STS proteome are scarce though some protein targets are amenable to clinical diagnostic application through immunohistochemistry (12,13). mRNAs expression levels and corresponding proteins profiles do not necessarily correlate well, which suggests a complex interplay between copy number and protein abundance (14). Additionally, factors such as post-translational modifications, compartmentalization and relative synthesis and degradation rates, play an important role in protein function. In order to profile protein expression in UPS and LMS, we used nano-flow liquid chromatography coupled with tandem mass spectrometry and performed quantitative protein data analysis to highlight pathways with differential activity in order to define STS subsets.

Materials and Methods

Tumor samples and clinical pathological data

UPS and LMS of the extremities and the trunk wall were selected from the Lund Sarcoma Centre. The Lund University research ethics committee granted ethical permission for the study (LU302-02). Patients with metastases at diagnosis and those who had been treated with neoadjuvant chemo or radiotherapy were excluded. All tumors were reviewed by two experienced sarcoma pathologists, Dr. Pehr Rissler at Lund University Hospital and Dr. Jonathon Fletcher at Harvard Medical School, according to the WHO classification (15). Data on histo-pathological grade, necrosis, vascular invasion, depth, and size were collected in a standardized manner (Table 1).

LMS diagnosis required the presence of eosinophilic spindle cells with vesicular, blunt-ended, intended, or lobulated nuclei arranged in a fascicular pattern, accounting for 5–10% of the surface area examined. Tumors with these characteristics were also required to show unequivocal positivity for smooth-muscle actin (SMA) as well as for desmin and/or h-caldesmon. MFH/UPS were defined as pleomorphic spindle-cell sarcomas without any specific differentiation. These tumors were also negative for melanocytic and hematopoietic markers. Adequate tissue samples and clinical data were available from all cases. Myofibroblastic sarcoma was a pleomorphic spindle-cell sarcoma with either storiform or fascicular growth patterns composed mainly of cells with pale or moderately eosinophilic cytoplasm (without sharply defined cell borders) and pointed, tapering, or somewhat wavy hyperchromatic nuclei. In undoubted cases, there was always widespread positivity for HHF-35 or SMA but not for desmin, and the nuclear features were not convincing for leiomyosarcoma.

Tumour blocks were obtained with 1cm intervals from the entire specimen and all available blocks were analysed using 4μm sections. All tumours were stained at the Department of Pathology, Skåne University Hospital, Lund.

Materials and Reagents

Chemicals (Urea, CHAPS, Tris, glycerol, magnesium acetate, ammonium bicarbonate, dithiothreitol,, iodoacetamide and bromophenol blue) and the total protein assay kit, micro-Lowry Peterson's modification, were purchased from Sigma Aldrich (Stockholm, Sweden). IPG ampholytes, immobilized pH gradient strips, SDS, and CyDyes were from GE Healthcare (Uppsala, Sweden). Sequencing-grade modified trypsin was from Promega Biotech AB (Stockholm, Sweden). 2x Laemmli sample buffer, and 12% Criterion TGX precast gels were from Bio-Rad laboratories Inc. (Hercules, CA, USA). GelCode Blue Stain reagent, and Zeba protein desalting spin columns were from Pierce Biotechnology (Rockford, IL, USA). Formic acid was from JT Baker (Philipsburg, NJ, USA). HPLC grade acetonitrile, and water were from Fluka analytical (Sigma Aldrich, Stockholm, Sweden). Ultramicrospin C18 columns were from the Nest Group (Southborough, MA, USA), and the SCX column was from Applied Biosystems, Foster City, CA, USA. The TMT labeling kit was from Pierce Biotechnology (Rockford, IL, USA).

Protein Extraction from Tissue

Tissues were collected after surgery at the orthopedic unit, Lund University Hospital and made anonymous after informed consent and approval by the ethics committee. 139 samples of all types of STS were selected including 16 UPS and 38 LMS tumors. The resected sample was put on ice and a pathologist first examined all samples to obtain representative, viable, and non-necrotic tumor tissue, which was then snap frozen. 250mg frozen tumor tissue was used for sample preparation for proteomics analysis. The tissue was put in a grinding beaker together with a steel ball and immersed in liquid nitrogen. After this step, the tumor was ground for 30 seconds in a micro-dismembrator II operating at 60 strokes per second at maximal amplitude, refrozen in liquid nitrogen and then ground again for 30 seconds.

2D DIGE Analysis

The protein extracts were thawed on ice in lysis buffer containing 8 M urea, 30 mM Tris, 5 mM magnesium acetate, 4% CHAPS, pH 8.5. 38 of the samples were extremely viscous and could not be pipetted even after sonication and DNase treatment and were removed from the study. The protein concentrations of the remaining 101 samples were determined using the total protein micro-Lowry assay kit. All 101 samples were labeled with Cy3 and Cy5 independently, according to the manufacturer's protocol. A total of 200 pmol of dye per 25 µg of protein was used. Equal amounts of protein from each sample were mixed to form a pool. The pool was labeled with Cy2. After labeling the pool was divided into aliquots of 25 µg. The volumes of the labeled samples were adjusted to 20 µl with magnesium lysis buffer, and 20-µl 2x sample buffer (8 M urea, 130 mM DTT, 4% CHAPS, 2% IPG ampholytes) was added. A Cy3 labeled sample, a Cy5 labeled sample and a Cy2 labeled aliquot of the pool were combined and mixed with 330 µl rehydration buffer (8 M urea, 2% CHAPS, 0.002% bromophenol blue, 2.8 mg/ml DTT, 0.5% IPG ampholytes). The samples were left at room temperature for 30 min, centrifuged for 30 min at 16.200 rpm before loading onto a 24 cm immobilized pH gradient strip (pH 4-7) for 14 hours rehydration.

First-dimension isoelectric focusing was carried out on an Amersham Biosciences IPG-phor with a total focusing time of 67 kVh. Before the second-dimension separation the strips were incubated in 20 ml equilibration solution (6 M urea, 75 mM Tris (pH 8.8) 30% (w/v) glycerol, 2% (w/v) SDS, 0.002% bromophenol blue) supplemented with 10 mg/ml DTT for 15 min, followed by 15 min incubation in equilibration buffer supplemented with 25 mg/ml iodoacetamide. The IPG strips were then loaded and run on 12.5% SDS-PAGE for 3 hours at 10 W/gel. The gels were fixed in 30% ethanol and 10% acetic acid for 30 min, and then kept in water. The gels were scanned with an Amersham Biosciences Typhoon 9400 variable imager. Spot detection and matching was carried out in Progenesis Samespots using on average 10 manual landmarks.

Label-free Quantification

The overall experimental flow design is shown in supplementary figure 5. Twenty UPS and LMS samples were selected based on the results from the 2D-gel analysis for in depth analysis. 100 µg of protein from each of the selected samples were mixed 1:1 with 2x Laemmli sample buffer, heated for 5 min at 95°C and subsequently run shortly into 12% Criterion TGX precast gels at a constant current of 25 mA/gel at 25°C. The run was stopped as the front entered 3 mm into the resolving gel, so that the entire protein extract was concentrated in the stacking/resolving gel interface. The protein bands were visualized using GelCode Blue Stain reagent, excised and cut into 2 x 2 mm cubes, and in-gel digested essentially according to the method by Wilm et al. (16).

Briefly, the gel pieces were de-stained repeatedly in 50% acetonitrile in 50 mM ammonium bicarbonate and 100 mM ammonium bicarbonate and then dehydrated using 100% acetonitrile and dried in a vacuum centrifuge. The disulfide bonds were reduced with 20 mM DTT in 100 mM ammonium bicarbonate for 1 hour at 56°C and subsequently alkylated using 55 mM iodoacetamide in 100 mM ammonium bicarbonate for 45 min at room temperature in the dark. After washing with 50% acetonitrile in 50 mM ammonium bicarbonate the gel pieces were dehydrated in 100% acetonitrile and dried in a vacuum centrifuge. The gel pieces were re-swelled on ice for 45 min in digestion buffer containing 10 ng/µl sequencing-grade modified trypsin in 50 mM ammonium bicarbonate and then incubated at 37°C overnight. Peptides were extracted by incubating the gel pieces in 5% formic acid in

50% acetonitrile for 15 min. The extraction step was repeated three times and the peptide extracts were pooled and dried in a vacuum centrifuge, dissolved in 0.1% formic acid. Peptides were cleaned up using Ultramicrospin C18 columns according to the manufacturer's instructions. The eluted peptides were dried in a vacuum centrifuge, dissolved in 0.1% formic acid and stored at -20°C until analysis by RP-HPLC MS/MS. 1 µg of each sample was infused into the mass spectrometer in duplicates for the analysis.

TMT Quantification

For Tandem Mass Tag labeling, a reference sample was prepared from mixing equal amounts of the twenty selected samples (see above). 100 µg of protein from each of the twenty samples and four aliquots of 100 µg of protein from the reference sample were run shortly into gels, in-gel digested as described for the label-free analysis. The peptides extracted from the gels were resuspended in 100 µl 200 mM TEAB and the peptides were labeled with isobaric TMT reagents according to the manufacturer's protocol. The labeled samples were combined into four groups A-D. Each group was composed of five samples labeled with either TMT127-TMT131 together with a reference sample labeled with TMT126.

The four groups were subsequently cleaned and fractionated into eight fractions on a SCX column (ICAT, Strong Cation Exchange Cartridge) at a flow rate of 50 µl/min. The samples were loaded on the pre-equilibrated cartridge and then eluted in 500 µl fractions by injecting KCl at increasing concentrations (30, 60, 90, 120, 240, 300, 420, 500 mM) in 5 mM KH2PO4, 25% acetonitrile. The volume of the fractions was then reduced to less than 100 µl using a vacuum centrifuge. The fractions were desalted using Ultramicrospin C18 columns. The eluted peptides were dried in the vacuum centrifuge, dissolved in 0.1% formic acid and subsequently analyzed by RP-HPLC MS/MS.

Mass Spectrometry Analysis

An ESI-LTQ-Orbitrap XL mass spectrometer (Thermo Electron, Bremen, Germany) interfaced with an Eksigent nanoLC plus HPLC system (Eksigent technologies, Dublin, CA, USA) was used for all

analyses. Peptides were loaded a constant flow rate of 10 µl/min onto a pre-column (PepMap 100, C18, 5 µm, 5 mm x 0.3 mm, LC Packings, Amsterdam, Netherlands) and subsequently separated on a 10 µm fused silica emitter, 75 µm x 16 cm (PicoTip™ Emitter, New Objective, Inc. Woburn, MA, USA), packed in-house with Reprosil-Pur C18-AQ resin (3 µm Dr. Maisch GmbH, Ammerbuch-Entringen, Germany). Peptides were eluted with a 150 min (label-free quantification) or a 90 min (TMT quantification) linear gradient of 3 to 35% acetonitrile in water, containing 0.1% formic acid, with a flow rate of 300 nl/min.

The LTQ-Orbitrap was operated in a data-dependent mode simultaneously acquiring MS spectra in the Orbitrap (from m/z 400 to 2000) and MS/MS spectra in the LTQ. For the label-free analysis, four MS/MS spectra were acquired using CID (collision induced dissociation) in the LTQ and each Orbitrap-MS scan was acquired at 60,000 FWHM nominal resolution settings using the lock mass option (m/z 445.120025) for internal calibration. For the TMT quantification analysis the instrument selected three precursor ions for sequential fragmentation by CID and HCD (higher-energy collisional dissociation), for analysis in the LTQ and Orbitrap (recorded at a resolution of 15,000), respectively. The normalized collision energy was set to 35% for CID and 45% HCD. The dynamic exclusion list was restricted to 500 entries using a repeat count of two with a repeat duration of 20 seconds and with a maximum retention period 120 seconds. Precursor ion charge state screening was enabled to select for ions with at least two charges and rejecting ions with undetermined charge state.

Data analysis

Raw mass spectrometric data was independently analyzed in Progenesis LC-MS (Nonlinear Dynamics Ltd, version 4.1.4804) and Proteios SE (version 2.19.0)(17) software platforms. In both cases, runs were aligned and peptide identifications were propagated between runs in order to minimize missing values. MS/MS spectra of ions with charge +2/+3/+4 between 400-1000 m/z and 27-62 mins were filtered and submitted to Mascot for identification using the UniProt database release 2012 filtered for human. Identifications were filtered with an FDR of 0.05 at the peptide and protein levels. Only proteins with at least one unique peptide were kept in the dataset. Qlucore Omics Explorer (Qlucore AB, version 2.3) software was used for statistical analysis of the protein expression profiles. The

functional enrichment analysis was carried out with MetaCore™ (Thomson Reuters, version 6.14) and DAVID (National Institute of Allergy and Infectious Diseases NIH, version 6.7).

Results & Discussion

There was little overlap between these tumors and those that were used in the previous genomics study, which limited the value of a correlation analysis between the results from the two studies. Furthermore, the mRNA and proteomic samples from those few tumors that were included in both studies were taken from different regions of the tumor, which further limited the usefulness of a comparison. The gel study was carried out using tumour samples run in duplicate using dye swapping to balance out the different reactivities occasionally seen with the Cy3 and Cy5 dyes.

Unsupervised hierarchical clustering of the 139 tumors, based on 873 spots analyzed in 2D DIGE experiment revealed different protein expression profiles amongst the STS tumors but in general no strong clustering was observed (Supplementary data figure 1). The gels were aligned, matched and analysed by Progenesis SameSpots and statistical analysis was carried out in SameSpots and also using routines written in R. No significant clustering could be found by either Pearson correlation analysis nor by principal component analysis. A more focused analysis showed several clusters within the LMS samples, but which did not separate LMS samples from MFH/UPS (Figure 1). Based on the hierarchical clustering, we defined three LMS clusters and a forth cluster enriched for myogenic UPS, referred to as LMS_A, LMS_B and LMS_C, and UPS_D. From each cluster, five samples were selected for in depth analysis by HPLC-MS/MS using TMT-labeling (Figure 1).

1105 proteins were identified overall and 778 proteins were quantified in at least one group, using only unique peptides. Measurements within each subgroup were then taken as biological replicates to allow an inter-group analysis. Principal component analysis of the 778 proteins identified three proteins, vinculin (VCL), COL6A3 and MYH11 that discriminated between the groups in multi-group comparison with $R^2 \geq 0.9025$. Vinculin is a focal adhesion protein primarily involved in cell-

cell and cell-matrix adhesion. Focal adhesion proteins do not only regulate mechanical force transmission, but also indirectly modulate diverse cellular processes such as proliferation, differentiation, apoptosis and cell motility, via integrin signaling (18,19). Vinculin deregulation has been associated with malignant potential, tumorogenicity and metastatic potential (20,21). More specifically, a role for Vinculin in regulation of survival and motility via ERK(22), as well as its indirect control over PTEN activity via regulation of ß-catenin-MAGI2 interaction (23) has been reported. The *Col6a3* gene codes the alpha-3 chain of collagen type VI, a secreted protein primarily involved in the extracellular matrix (ECM). *Col6a3 gene* has been shown to undergo tumor-specific splice variation in several different malignancies such as colon, prostate and pancreatic cancer(24-26). In mesenchymal tumor cells, both vinculin and collagen type VI are known to be regulated (27,28). Furthermore, COL6A3 overexpression was shown to correlate well with both tumor grade and resistance to the chemotherapy agent cisplatin in ovarian cancer cells, pointing towards a significant ECM remodeling in these tumors (29). Finally, the *Myh11* gene codes for myosin heavy chain, smooth muscle isoform. To our knowledge this particular gene or the protein it encodes, have not been associated with pleomorphic STS. Considering that MYH11 is a commonly used marker for smooth-muscle tissue, it is likely that the difference in MYH11 expression we have observed points indicates the level of differentiation among the tumors in the study.

Pathway enrichment analysis of this data using MetaCore software identified “glycolysis and gluconeogenesis” pathway significantly enriched in the LMS groups (LMS-A, -B, and –C), whereas “cytoskeleton remodeling” and “cell adhesion” pathway were significantly enriched in the UPS group (UPS-D).

Label-free quantitative mass spectrometry reveals at least two distinct subgroups within LMS

Given the low overlap of proteins between the groups in the TMT analysis, we further analyzed each tumor sample using a label-free approach with two technical replicates. We identified >2500 proteins, of which 1632 were quantified with proteotypic peptides following chromatogram alignment using Progenesis LC-MS software. We initially examined whether protein expression profiles allowed the discrimination between LMS and UPS. Two-way comparison (LMS versus UPS) in Qlucore did not

result in a significant separation of samples (not shown), whereas multi-group comparison separated the groups (Figure 2a). Unsupervised hierarchical clustering based on variables that pass $q < 0.05$ threshold (Table 2) showed that Group-A LMS appear distinct from tumors in LMS-B and LMS-C, whereas group-D containing UPS did not show a distinct pattern (see Figure 2b) and appeared closer to A than to B and C. This interpretation is consistent with the PCA plot, where UPS group-D samples are spread over the axis of the first principal component between LMS-A, LMS-B and LMS-C. We therefore suggest that LMS encompass at least two subgroups with respect to protein expression profiles, whereas UPS are spread over the hypothetical space in between these two subgroups, thus suggesting a close relation between UPS and LMS.

We subsequently removed the UPS samples from the statistical analysis, and performed a two-way comparison analysis of samples in LMS group-A versus those in LMS groups B and C. Using the same significance criteria, the number of discriminating variables increased considerably resulting in 156 proteins, see Figure 3 and Table 3. We investigated the functional annotations associated with these proteins using the DAVID tool (30) and found out a large group of ribosomal proteins, together with subunits of eukaryotic translation initiation factors (eIF). Consequently, protein biosynthesis and translation were the most significant functional terms indicating that LMS-A probably has a higher level of protein production compared to LMS-B and LMS–C. The distinction between LMS-B and LMS–C is less clear however. With the same significance measure ($q < 0.05$), no protein in our dataset could discriminate between the two groups. Even with less stringent selection criteria, the remaining proteins did not yield a meaningful functional enrichment. We believe this is due to intra-group variability and that it warrants further studies into protein expression of group-B and group-C LMS. It is also worth considering the possibility that the distinction between these two groups is insignificant and that there are essentially two subgroups of LMS and not three.

Pathway analysis of the subgroups

In order to identify differentially regulated pathways, we have used the list of 156 proteins that discriminate LMS-A from LMS-B and LMS-C. This revealed several significant pathways such as "apoptosis and survival: Granzyme A signaling" (Supplementary Figure 2), "cytoskeleton

remodeling" (Supplementary Figure 3), as well as "telomere regulation and cellular immortalization" (Supplementary Figure 4). One of the most significantly differing proteins in Granzyme A signaling pathway was Prelamin-A/C, coded by the LMNA gene (Figure 4). Lamin family proteins are components of the nuclear lamina, which in turn provides support to the nucleus and are central to maintenance of nuclear integrity. It has been shown in literature that lamins may play an important role in chromatin organization and telomere dynamics (31). Furthermore, it is suggested that Prelamin-A/C accumulation plays a role in smooth-muscle cell senescence by disrupting mitosis and inducing DNA damage in vascular smooth-muscle cells causing genomic instability and premature senescence. Additionally, Prelamin-A/C accumulation appears to deregulate the G2/M checkpoint (32).

We also observed differential expression of the Ku70 protein, which is involved in telomere regulation and cellular immortalization, with an average overexpression of 2.5 in LMS-A compared to LMS-B and LMS-C. Ku70 protein is one of the two subunits of the Ku complex in which ATP-dependent helicase is known to play an important role in the non-homologous end joining (NHEJ) pathway as well as telomere regulation (33,34).

Potential biomarkers for vascular invasion in soft-tissue sarcomas

Vascular invasion is a negative prognostic factor in STS, which motivated assessment of protein profiles in the STS that showed vascular invasion. Two-way comparison in Qlucore Omics Explorer with filtered variables ($p < 0.001$) that discriminate between the two groups identified three significantly deregulated proteins (Figure 5); Vinculin (VINC), Intergrin-linked protein kinase (ILK) and Creatine kinase type B (CKB). We have shown above that Vinculin is a key player in cell adhesion. Additionally, elevated Vinculin levels have been associated with angiogenesis (35,36). The correlation between metastasis, angiogenesis and ILK signaling has been addressed in various malignancies (37-40), including osteosarcoma (41) and chondrosarcoma (42). The alpha-parvin (PARVA) protein, which interacts with ILK is differentially expressed ($p = 0.0012$). PARVA plays a role in smooth-muscle contraction, as well as in angiogenic sprouting and adhesion between smooth-muscle cells and endothelial cells during vessel development (43-45). Furthermore, the significance of the expression regulation of ILK and its partners was previously studied in chondrosarcomas (46). It is

important to note however that our sample size is small with respect to tumors showing vascular invasion (n = 4) and thus our dataset is not large enough to draw strong conclusions.

Conclusions

Our analysis has shown that LMS, in agreement with previous gene expression studies, could be divided into three subgroups, with distinct proteomic profiles. One of the subgroups, referred to as group-A LMS, displayed a strikingly distinct protein profile and was enriched for ribosomal proteins as well as eukaryotic translation initiation factors. These findings, at a proteomic level, are in line with previous expression studies that confirm LMS complexity. In general, the protein profiles do not correlate well with the gene expression profiles due to temporal differences in expression and turnover. In our study we found that several proteins, including ARPC3, UB2D3, DDX17 and PHB2, all up-regulated in group-A LMS, as well as LMNA, which is down-regulated in group-A LMS, can be used to discriminate group-A LMS from other types of LMS. Pathway analysis of our dataset indicated that apoptosis and survival (particularly Granzyme A signaling) cytoskeleton remodeling and telomere maintenance/regulation to be likely candidates for differential regulation between the LMS subgroups.

Our results also indicate that expression regulation of several key proteins, in particular VCL and COL6A3, might play important roles in the progression of pleomorphic STS. Specifically their role in the ECM and cell adhesion warrants future studies on expression levels of these proteins, and their associates, in tumor invasiveness and metastatic potential. Differential MYH11 expression on the other hand, could be useful in determination of the differentiation state of the tumors.

We have also addressed the relationship and similarity between UPS and LMS. We have previously performed a comparison of UPS/LMS at a genetic/gene expression level suggesting that UPS could indeed correspond to highly pleomorphic LMS. In this study UPS appeared to spread out in the PCA analysis and cluster in between the LMS subgroups in unsupervised clustering. This

reinforces the concept that UPS and LMS may represent a common lineage at different differentiation stages. Mesenchymal stem cells (MSCs) have been shown to be the likely origin of MFH/UPS tumors and the role of Wnt signaling in commitment to differentiation has been highlighted (8). Furthermore, a recent study has shown that both types of tumors (UPS and LMS) can originate from the same *Pten*/*p53* inactivated murine model, which also points towards shared lineage between these histotypes (47). In this light, tumors classified as MFH/UPS originate from different time points along smooth-muscle differentiation of hMSCs, and represent different steady (or semi-steady) states of gene expression based on other relevant mutations that might have been accumulated or inherited. Thus we conclude that this discovery phase experiment using first 2D-PAGE, then two independent LC-MS analyses, label-free and isotopic labeling has provided compelling evidence that there are indeed subtypes to be found in the UPS and LMS sarcomas. The distinct lack of clustering in the majority of tumor types indicates the extent of the heterogeneity in this cancer type and the need for individual analyses of each patient tumor to define the type of aberration that has led to development of the tumor and possibly indicate how it should be treated. This discovery phase experiment has opened the way for a future independent validation using new tumor sets. The proteins we have identified here as differentially expressed among the subgroups may play a relevant biological role to be addressed in further studies.

Acknowledgements

We would like to thank Josefin Fernebro, Emelie Styring, Anders Rydholm, Fredrik Vult von Steyern, Pehr Rissler for contributing with tumor samples and clinical pathological data, as well as Liselotte Andersson and Fredrik Levander for their help and support throughout the project.

The mass spectrometry proteomics data have been deposited to the ProteomeXchange Consortium (http://proteomecentral.proteomexchange.org) via the PRIDE partner repository [1] with the dataset identifiers PXD000616 and PXD000617. We would like to extend our thanks to PRIDE Team for their help in making the dataset available. This project was supported by grants from Swedish National Research Council (VR-NT, PJ), the Foundation for Strategic Research (SSF; PJ) (Strategic Centre for Translational Cancer Research - CREATE Health), the Knut and Alice Wallenberg

foundation (PJ) and Vinnova (PJ) as well as Swedish Cancer Fund (MN), the Nilsson Cancer Fund (MN) and Yngre ALF 2013-2015 (AC).

Tables

Table 1. A listing of leiomyosarcoma and myogenic sarcomas covered in this study. Age column refers to age at diagnosis and tumor size is given in cm (diameter).

Id	Histotype	Group	Age	necrosis	vascular invasion	tumor size	grade
LMS_101	Leiomyosarcoma		78	yes	no	20	High grade
LMS_102	Leiomyosarcoma	C	81	yes	no	7	High grade
LMS_103	Leiomyosarcoma	A	57	no	no	8	High grade
LMS_123	Leiomyosarcoma	C	88	yes	no	11	High grade
LMS_124	Leiomyosarcoma	C	75	yes	no	4	High grade
LMS_126	Leiomyosarcoma	B	72	yes	yes	5	High grade
LMS_127	Leiomyosarcoma		79	yes	yes	16	High grade
LMS_133	Leiomyosarcoma	B	81	yes	no	7	High grade
LMS_14	Leiomyosarcoma		76	yes	no	7	High grade
LMS_15	Leiomyosarcoma	A	83	yes	yes	17	High grade
LMS_17	Leiomyosarcoma	A	80	yes	yes	11	High grade
LMS_26	Leiomyosarcoma	A	64	yes	no	9	High grade
LMS_27	Leiomyosarcoma	A	82	yes	yes	11	High grade
LMS_32	Leiomyosarcoma		96	yes	no	20	High grade
LMS_37	Leiomyosarcoma		56	yes	no	4	High grade
LMS_40	Leiomyosarcoma	B	54	yes	no	4	High grade
LMS_44	Leiomyosarcoma		77	yes	no	6	High grade
LMS_46	Leiomyosarcoma	C	84	no	no	5	High grade
LMS_47	Leiomyosarcoma	C	54	yes	no	14	High grade
LMS_49	Leiomyosarcoma		54	yes	yes	7	High grade
LMS_5	Leiomyosarcoma	B	61	yes	no	6	High grade
LMS_6	Leiomyosarcoma	B	80	yes	yes	6	High grade
LMS_65	Leiomyosarcoma		79	yes	no	12	High grade
LMS_7	Leiomyosarcoma		74	yes	yes	3	High grade
LMS_8	Leiomyosarcoma		82	yes	no	9	High grade
LMS_95	Leiomyosarcoma		94	yes	no	18	High grade
MYO_134	Myogenic sarcoma	D	68	no	no	6	High grade
MYO_136	Myogenic sarcoma	D	78	no	no	7	High grade
MYO_60	Myogenic sarcoma	D	73	yes	no	30	High grade
MYO_67	Myogenic sarcoma	D	51	no	yes	8	High grade
MYO_68	Myogenic sarcoma	D	82	no	no	10	High grade

Table 2. A list of 20 proteins that discriminate between the 20 sarcomas in a multi-group comparison.

Description	p-value	q-value
ARPC3_HUMAN Actin-related protein 2/3 complex subunit 3	0.000325265	0.045337692
NU155_HUMAN Nuclear pore complex protein Nup155	0.000399275	0.045337692
RSSA_HUMAN 40S ribosomal protein SA	0.000499789	0.045337692
RL5_HUMAN 60S ribosomal protein L5	0.000598957	0.048790224
UB2D3_HUMAN Isoform 2 of Ubiquitin-conjugating enzyme E2 D3	2.92E-05	0.023866407
RS18_HUMAN 40S ribosomal protein S18	0.000627815	0.048790224
RL23A_HUMAN 60S ribosomal protein L23a	0.000472503	0.045337692
RL8_HUMAN 60S ribosomal protein L8	0.000439614	0.045337692
GBLP_HUMAN Guanine nucleotide-binding protein subunit beta-2-like 1	7.43E-05	0.033720688
SET_HUMAN Protein SET	0.000527829	0.045337692
FABP5_HUMAN Fatty acid-binding protein, epidermal	0.000320534	0.045337692
NU160_HUMAN Nuclear pore complex protein Nup160	0.000514988	0.045337692
AIMP2_HUMAN Aminoacyl tRNA synthase complex-interacting multifunctional protein	0.000411886	0.045337692

2		
SRSF6_HUMAN Serine/arginine-rich splicing factor 6	0.000349598	0.045337692
NACA_HUMAN Isoform 2 of Nascent polypeptide-associated complex subunit alpha	0.000315781	0.045337692
CAPR1_HUMAN Caprin-1	6.69E-06	0.010917141
PSMD6_HUMAN 26S proteasome non-ATPase regulatory subunit 6	0.000485567	0.045337692
SRSF7_HUMAN Serine/arginine-rich splicing factor 7	0.000182123	0.045337692
NUD13_HUMAN Nucleoside diphosphate-linked moiety X motif 13	0.000122145	0.039867986
DDX17_HUMAN Probable ATP-dependent RNA helicase DDX17	8.26E-05	0.033720688

Table 3. Top discriminators between Group-A vs. Group-B/-C leiomyosarcomas based on label-free MS/MS analysis.

Accession	Description	t-Statistic	p-value	q-value
O15145	ARPC3_HUMAN	6.690391064	1.49E-05	0.011147884
P61077-2;P61077-3;P62837;P62837-2	UB2D3_HUMAN	7.108072281	7.96E-06	0.011147884
Q92841;Q92841-1;Q92841-2	DDX17_HUMAN	6.23281765	3.05E-05	0.011147884
Q99623	PHB2_HUMAN	6.46544075	2.11E-05	0.011147884
Q01469	FABP5_HUMAN	6.03785944	4.18E-05	0.011371082
O75694	NU155_HUMAN	5.678377151	7.56E-05	0.013915789
O96019	ACL6A_HUMAN	5.47668457	0.000106278	0.013915789
P62750	RL23A_HUMAN	5.429849148	0.000115113	0.013915789
P62917	RL8_HUMAN	5.761602402	6.58E-05	0.013915789
P63244	GBLP_HUMAN	5.441791058	0.000112789	0.013915789
P84077;P61204	ARF1_HUMAN	5.408579826	0.000119376	0.013915789
Q13155	AIMP2_HUMAN	5.472631454	0.000107013	0.013915789
Q86X67	NUD13_HUMAN	5.543441296	9.49E-05	0.013915789
O14744	ANM5_HUMAN	5.347603798	0.000132539	0.014420204
P62269	RS18_HUMAN	5.161778927	0.000182873	0.015924926
Q14444	CAPR1_HUMAN	5.189430237	0.000174267	0.015924926
Q15185	TEBP_HUMAN	5.153915882	0.0001854	0.015924926
Q16629;Q16629-2;Q16629-3	SRSF7_HUMAN	5.177271366	0.000177998	0.015924926
P63241-2	IF5A1_HUMAN	5.002296448	0.00024197	0.018804551
Q99877;O60814;P58876;P62807;Q96A08	H2B1N_HUMAN	5.003736973	0.000241355	0.018804551
P46777	RL5_HUMAN	4.913110256	0.000283409	0.020109696
Q15008	PSMD6_HUMAN	4.931565762	0.000274265	0.020109696
P35232	PHB_HUMAN	4.81364584	0.000338462	0.023015425
P20645	MPRD_HUMAN	4.768265247	0.000367172	0.023566613
P35268	RL22_HUMAN	4.755867004	0.000375448	0.023566613

Figure captions

Figure 1: Unsupervised hierarchical clustering of LMS, MFH/UPS and NOS, based on the 2D-PAGE expression analysis. The 20 tumors chosen for further analysis are highlighted in light blue, yellow, pink and light green, corresponding with TMT pools A, B, C and D respectively.

Figure 2: (a) PCA plot of protein expression patterns of the 20 tumors, color coded and filtered for variables with $q < 0.05$. It is worth noting that 80% of the variability in the dataset is across the first principal component. Group-A LMS is separated from the other two groups of LMS along this axis with UPS samples occupying the space in between. The color-coding is: Group-A LMS: blue, Group-B LMS: yellow, Group-C LMS: pink, UPS-D: green. **(b)** A heat-map of 21 variables that satisfy $q < 0.05$ in a multi-group comparison analysis, overlaid with clinical variables such as necrosis and vascular invasion, as well as subtype information (color coding: Group-A LMS: blue, Group-B LMS: yellow, Group-C LMS: pink, UPS-D: green). Note that the last variable is a decoy hit

Figure 3: Heat map and hierarchical clustering of the proteins discriminating Group-A samples from the other leiomyosarcomas based on label-free LC-MS/MS analysis (color coding: Group-A LMS: blue, Group-B LMS: yellow, Group-C LMS: pink). The analysis is carried out as a two-way comparison in Qlucore Omics Explorer software with a threshold of $q < 0.05$.

Figure 4: The expression of Prelamin-A/C (LMNA_HUMAN) in studied LMS subgroups based on label-free LC-MS/MS analysis. Within the subset of 156 discriminators, LMNA is one of the few proteins that are under-expressed in LMS-A subgroup compared to LMS-B and LMS-C ($q \approx 0.027$), see Table 2.

Figure 5: Heat map and hierarchical clustering of the discriminating proteins between tumors annotated with positive vs. negative vascular invasion status, based on label-free LC-MS/MS analysis carried out as a two-way comparison in Qlucore Omics Explorer software, variables filtered for statistical threshold $p < 0.001$. (Color coding: Group-A LMS: blue, Group-B LMS: yellow, Group-C

LMS: pink, UPS-D: green. Maroon is used to annotate the samples with vascular invasion, light blue denotes for tumors that explicitly state no vascular invasion status and black denotes a missing annotation.)

References

1. van de Rijn M, Fletcher JA. Genetics of soft tissue tumors. Annu Rev Pathol. 2006;1:435–66.

2. Potter DA, Kinsella T, Glatstein E, Wesley R, White DE, Seipp CA, et al. High-grade soft tissue sarcomas of the extremities. Cancer. 1986;58:190–205.

3. Wardelmann E, Schildhaus H-U, Merkelbach-Bruse S, Hartmann W, Reichardt P, Hohenberger P, et al. Soft tissue sarcoma: from molecular diagnosis to selection of treatment. Pathological diagnosis of soft tissue sarcoma amid molecular biology and targeted therapies. Ann. Oncol. 2010;21 Suppl 7:vii265–9.

4. Nielsen TO, West RB, Linn SC, Alter O, Knowling MA, O'Connell JX, et al. Molecular characterisation of soft tissue tumours: a gene expression study. Lancet. 2002;359:1301–7.

5. Ren B, Yu YP, Jing L, Liu L, Michalopoulos GK, Luo J-H, et al. Gene expression analysis of human soft tissue leiomyosarcomas. Hum. Pathol. 2003;34:549–58.

6. Baird K, Davis S, Antonescu CR, Harper UL, Walker RL, Chen Y, et al. Gene expression profiling of human sarcomas: insights into sarcoma biology. Cancer Research. 2005;65:9226–35.

7. Nakayama R, Nemoto T, Takahashi H, Ohta T, Kawai A, Seki K, et al. Gene expression analysis of soft tissue sarcomas: characterization and reclassification of malignant fibrous histiocytoma. Mod. Pathol. 2007;20:749–59.

8. Matushansky I, Hernando E, Socci ND, Mills JE, Matos TA, Edgar MA, et al. Derivation of sarcomas from mesenchymal stem cells via inactivation of the Wnt pathway. J Clin Invest. 2007;117:3248–57.

9. Carneiro A, Francis P, Bendahl P-O, Fernebro J, Akerman M, Fletcher C, et al. Indistinguishable genomic profiles and shared prognostic markers in undifferentiated pleomorphic sarcoma and leiomyosarcoma: different sides of a single coin? Lab. Invest. 2009;89:668–75.

10. Beck AH, Lee C-H, Witten DM, Gleason BC, Edris B, Espinosa I, et al. Discovery of molecular subtypes in leiomyosarcoma through integrative molecular profiling. Oncogene. 2010;29:845–54.

11. Rubin BP, Nishijo K, Chen H-IH, Yi X, Schuetze DP, Pal R, et al. Evidence for an unanticipated relationship between undifferentiated pleomorphic sarcoma and embryonal rhabdomyosarcoma. Cancer Cell. 2011;19:177–91.

12. Suehara Y, Kondo T, Fujii K, Hasegawa T, Kawai A, Seki K, et al. Proteomic signatures corresponding to histological classification and grading of soft-tissue sarcomas. Proteomics. 2006;6:4402–9.

13. Kawai A, Kondo T, Suehara Y, Kikuta K, Hirohashi S. Global protein-expression analysis of bone and soft tissue sarcomas. Clin. Orthop. Relat. Res. 2008;466:2099–106.

14. Schwanhäusser B, Busse D, Li N, Dittmar G, Schuchhardt J, Wolf J, et al. Global quantification of mammalian gene expression control. Nature. 2011;473:337–42.

15. Fletcher CDM, Unni KK, Mertens F. Pathology & Genetics. IARC; 2002.

16. Wilm M, Shevchenko A, Houthaeve T, Breit S, Schweigerer L, Fotsis T, et al. Femtomole sequencing of proteins from polyacrylamide gels by nano-electrospray mass spectrometry. Nature. 1996;379:466–9.

17. Häkkinen J, Vincic G, Månsson O, Wårell K, Levander F. The proteios software environment: an extensible multiuser platform for management and analysis of proteomics data. J. Proteome Res. 2009;8:3037–43.

18. Critchley DR. Focal adhesions - the cytoskeletal connection. Curr. Opin. Cell Biol. 2000;12:133–9.

19. Desgrosellier JS, Cheresh DA. Integrins in cancer: biological implications and therapeutic opportunities. Nat Rev Cancer. 2010;10:9–22.

20. Rodríguez Fernández JL, Geiger B, Salomon D, Sabanay I, Zöller M, Ben-Ze'ev A. Suppression of tumorigenicity in transformed cells after transfection with vinculin cDNA. J. Cell Biol. 1992;119:427–38.

21. Goldmann WH, Auernheimer V, Thievessen I, Fabry B. Vinculin, cell mechanics and tumour cell invasion. Cell Biol. Int. [Internet]. 2013;37:397–405. Available from: http://onlinelibrary.wiley.com/doi/10.1002/cbin.10064/full

22. Subauste MC, Pertz O, Adamson ED, Turner CE, Junger S, Hahn KM. Vinculin modulation of paxillin-FAK interactions regulates ERK to control survival and motility. J. Cell Biol. 2004;165:371–81.

23. Subauste MC, Nalbant P, Adamson ED, Hahn KM. Vinculin controls PTEN protein level by maintaining the interaction of the adherens junction protein beta-catenin with the scaffolding protein MAGI-2. J. Biol. Chem. 2005;280:5676–81.

24. Gardina PJ, Clark TA, Shimada B, Staples MK, Yang Q, Veitch J, et al. Alternative splicing and differential gene expression in colon cancer detected by a whole genome exon array. BMC Genomics. 2006;7:325.

25. Thorsen K, Sørensen KD, Brems-Eskildsen AS, Modin C, Gaustadnes M, Hein A-MK, et al. Alternative splicing in colon, bladder, and prostate cancer identified by exon array analysis. Molecular & Cellular Proteomics. 2008;7:1214–24.

26. Arafat H, Lazar M, Salem K, Chipitsyna G, Gong Q, Pan T-C, et al. Tumor-specific expression and alternative splicing of the COL6A3 gene in pancreatic cancer. Surgery. 2011;150:306–15.

27. Schreier T, Friis RR, Winterhalter KH, Trüeb B. Regulation of type VI collagen synthesis in transformed mesenchymal cells. Biochem. J. 1988;253:381–6.

28. Schenker T, Trüeb B. Down-regulated proteins of mesenchymal tumor cells. Exp. Cell Res. 1998;239:161–8.

29. Sherman-Baust CA, Weeraratna AT, Rangel LBA, Pizer ES, Cho KR, Schwartz DR, et al. Remodeling of the extracellular matrix through overexpression of collagen VI contributes to cisplatin resistance in ovarian cancer cells. Cancer Cell. 2003;3:377–86.

30. Huang DW, Sherman BT, Lempicki RA. Systematic and integrative analysis of large gene lists using DAVID bioinformatics resources. Nat Protoc. 2009;4:44–57.

31. De Vos WH, Houben F, Hoebe RA, Hennekam R, van Engelen B, Manders EMM, et al. Increased plasticity of the nuclear envelope and hypermobility of telomeres due to the loss of A-type lamins. Biochim. Biophys. Acta. 2010;1800:448–58.

32. Ragnauth CD, Warren DT, Liu Y, McNair R, Tajsic T, Figg N, et al. Prelamin A acts to accelerate smooth muscle cell senescence and is a novel biomarker of human vascular aging. Circulation. 2010;121:2200–10.

33. Boulton SJ, Jackson SP. Components of the Ku-dependent non-homologous end-joining pathway are involved in telomeric length maintenance and telomeric silencing. EMBO J. 1998;17:1819–28.

34. Badie C, Yáñez-Muñoz RJ, Muller C, Salles B, Porter ACG. Impaired telomerase activity in human cells expressing GFP-Ku86 fusion proteins. Cytogenet. Genome Res. 2008;122:326–35.

35. Bernardo BC, Gao X-M, Winbanks CE, Boey EJH, Tham YK, Kiriazis H, et al. Therapeutic inhibition of the miR-34 family attenuates pathological cardiac remodeling and improves heart function. Proceedings of the National Academy of Sciences. 2012;109:17615–20.

36. Huveneers S, Oldenburg J, Spanjaard E, van der Krogt G, Grigoriev I, Akhmanova A, et al. Vinculin associates with endothelial VE-cadherin junctions to control force-dependent remodeling. J. Cell Biol. 2012;196:641–52.

37. Chang L-H, Pan S-L, Lai C-Y, Tsai A-C, Teng C-M. Activated PAR-2 Regulates Pancreatic Cancer Progression through ILK/HIF-α-Induced TGF-α Expression and MEK/VEGF-A-Mediated Angiogenesis. Am. J. Pathol. 2013.

38. Engelman M de FB, Grande RM, Naves MA, de Franco MF, de Paulo Castro Teixeira V. Integrin-linked kinase (ILK) expression correlates with tumor severity in clear cell renal carcinoma. Pathol. Oncol. Res. 2013;19:27–33.

39. Imanishi Y, Hu B, Jarzynka MJ, Guo P, Elishaev E, Bar-Joseph I, et al. Angiopoietin-2 stimulates breast cancer metastasis through the alpha(5)beta(1) integrin-mediated pathway. Cancer Research. 2007;67:4254–63.

40. Takanami I. Increased expression of integrin-linked kinase is associated with shorter survival in non-small cell lung cancer. BMC Cancer. 2005;5:1.

41. Rhee SH, Han I, Lee MR, Cho HS, Oh JH, Kim H-S. Role of integrin-linked kinase in osteosarcoma progression. J. Orthop. Res. 2013.

42. Wu M-H, Huang C-Y, Lin J-A, Wang S-W, Peng C-Y, Cheng H-C, et al. Endothelin-1 promotes vascular endothelial growth factor-dependent angiogenesis in human chondrosarcoma cells. Oncogene. 2013.

43. Olski TM, Noegel AA, Korenbaum E. Parvin, a 42 kDa focal adhesion protein, related to the

alpha-actinin superfamily. J. Cell. Sci. 2001;114:525–38.

44. Tu Y, Huang Y, Zhang Y, Hua Y, Wu C. A new focal adhesion protein that interacts with integrin-linked kinase and regulates cell adhesion and spreading. J. Cell Biol. 2001;153:585–98.

45. Zhang Y, Chen K, Tu Y, Wu C. Distinct roles of two structurally closely related focal adhesion proteins, alpha-parvins and beta-parvins, in regulation of cell morphology and survival. J. Biol. Chem. 2004;279:41695–705.

46. Papachristou DJ, Gkretsi V, Rao UNM, Papachristou GI, Papaefthymiou OA, Basdra EK, et al. Expression of integrin-linked kinase and its binding partners in chondrosarcoma: association with prognostic significance. Eur. J. Cancer. 2008;44:2518–25.

47. Guijarro MV, Dahiya S, Danielson LS, Segura MF, Vales-Lara FM, Menendez S, et al. Dual Pten/Tp53 suppression promotes sarcoma progression by activating Notch signaling. Am. J. Pathol. 2013;182:2015–27.

Author Manuscript Published OnlineFirst on July 28, 2014; DOI: 10.1158/1541-7786.MCR-14-0072

Figure 1

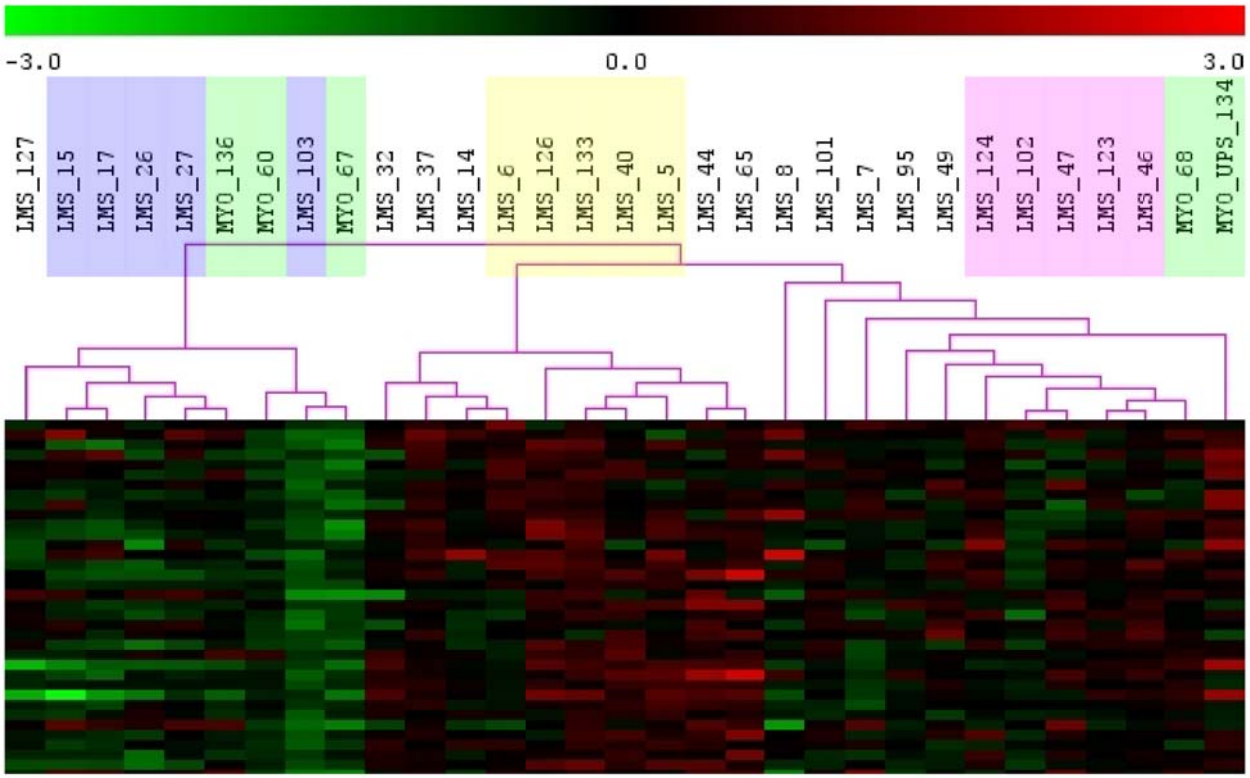

Author Manuscript Published OnlineFirst on July 28, 2014; DOI: 10.1158/1541-7786.MCR-14-0072

Figure 2

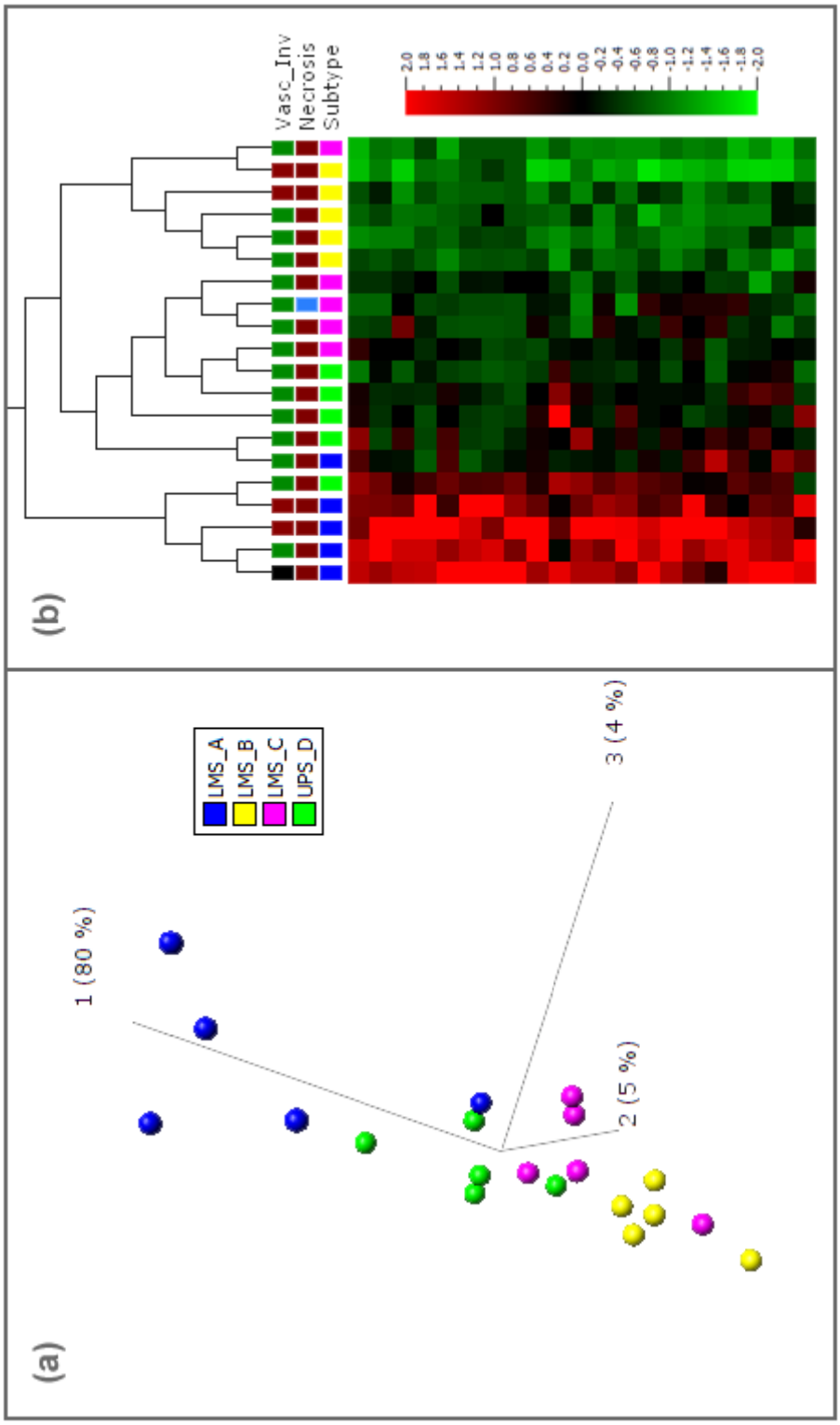

Figure 3

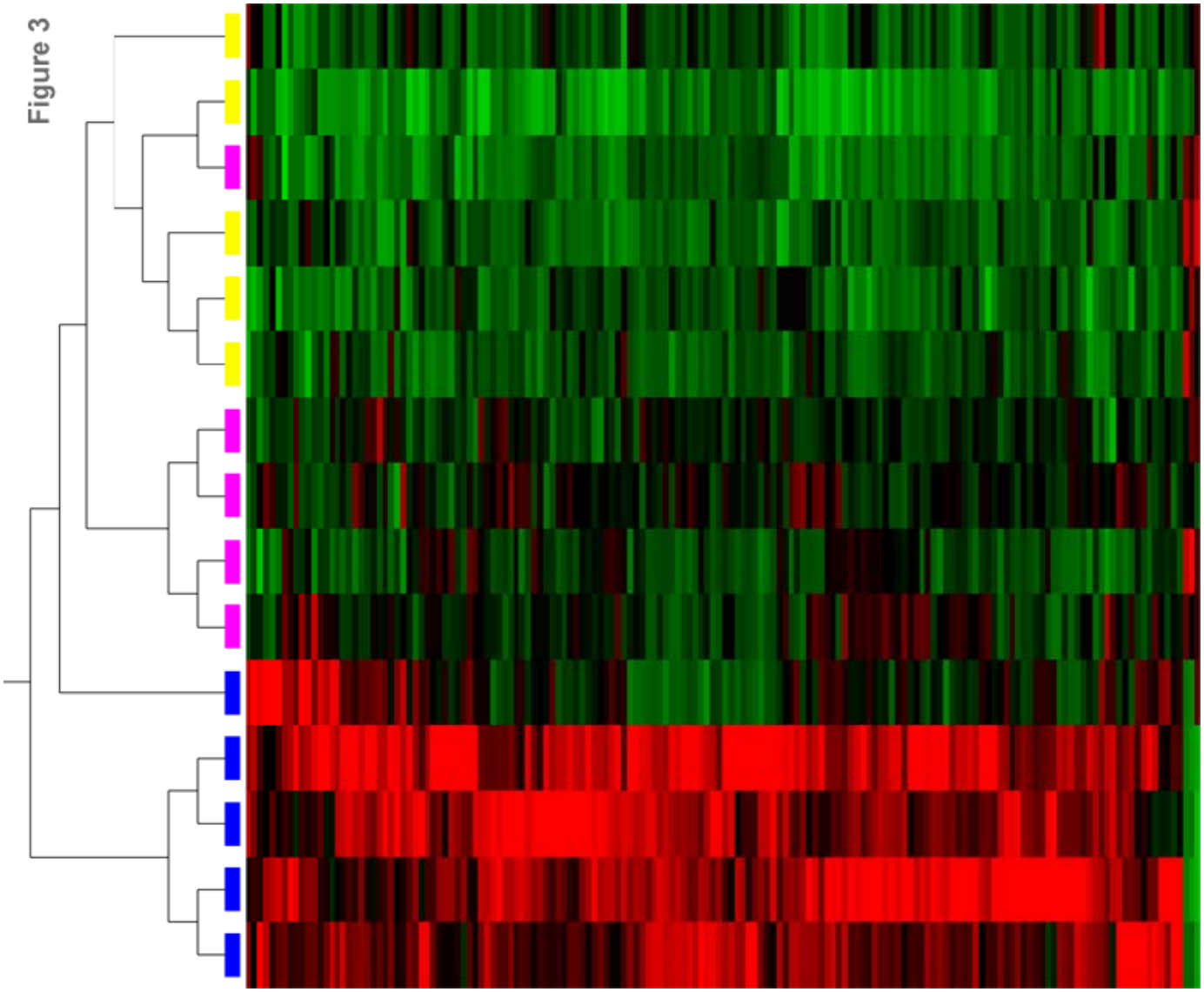

Author Manuscript Published OnlineFirst on July 28, 2014; DOI: 10.1158/1541-7786.MCR-14-0072
Author manuscripts have been peer reviewed and accepted for publication but have not yet been edited.

Figure 4

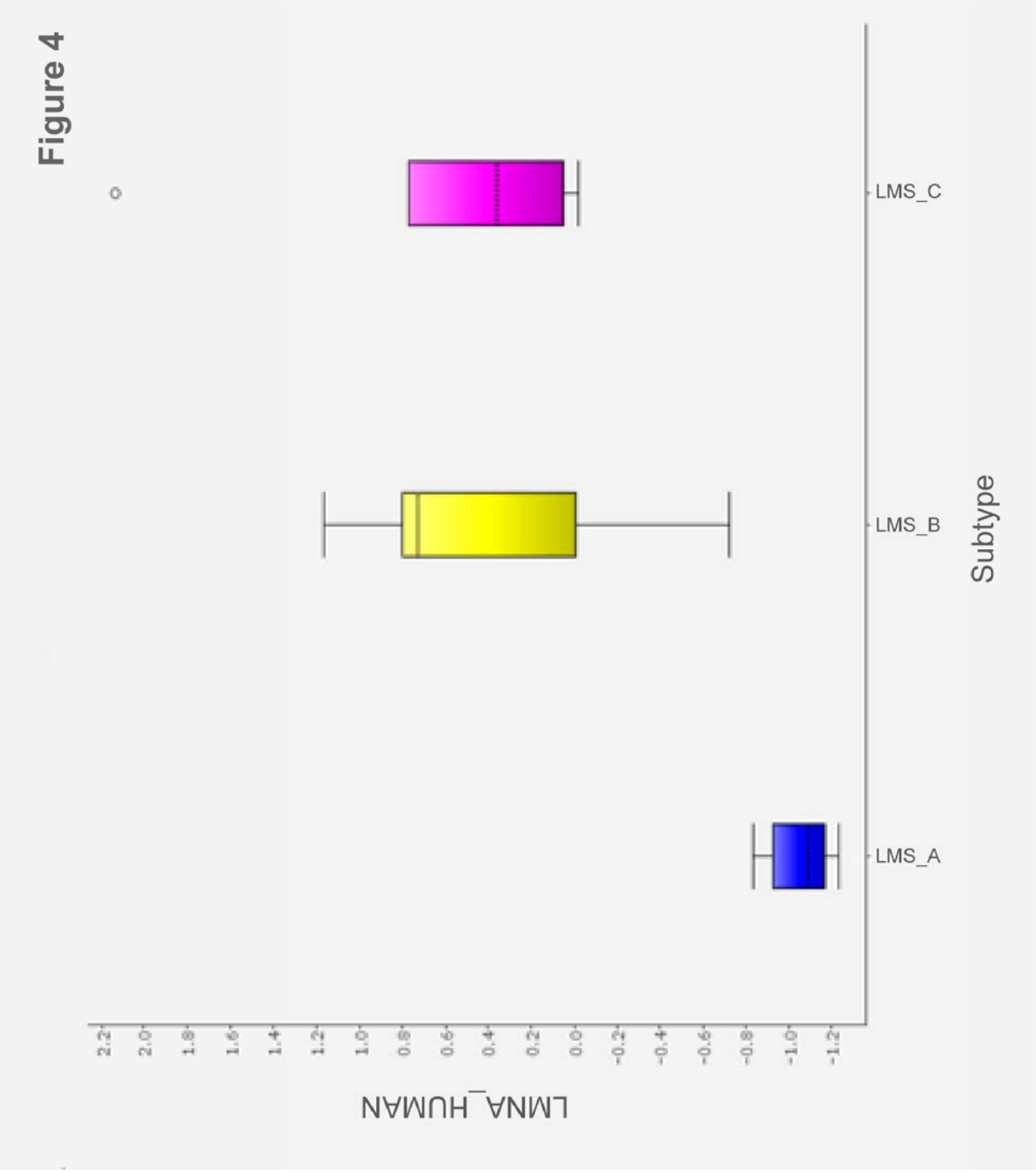

Author Manuscript Published OnlineFirst on July 28, 2014; DOI: 10.1158/1541-7786.MCR-14-0072
Author manuscripts have been peer reviewed and accepted for publication but have not yet been edited.

Figure 5

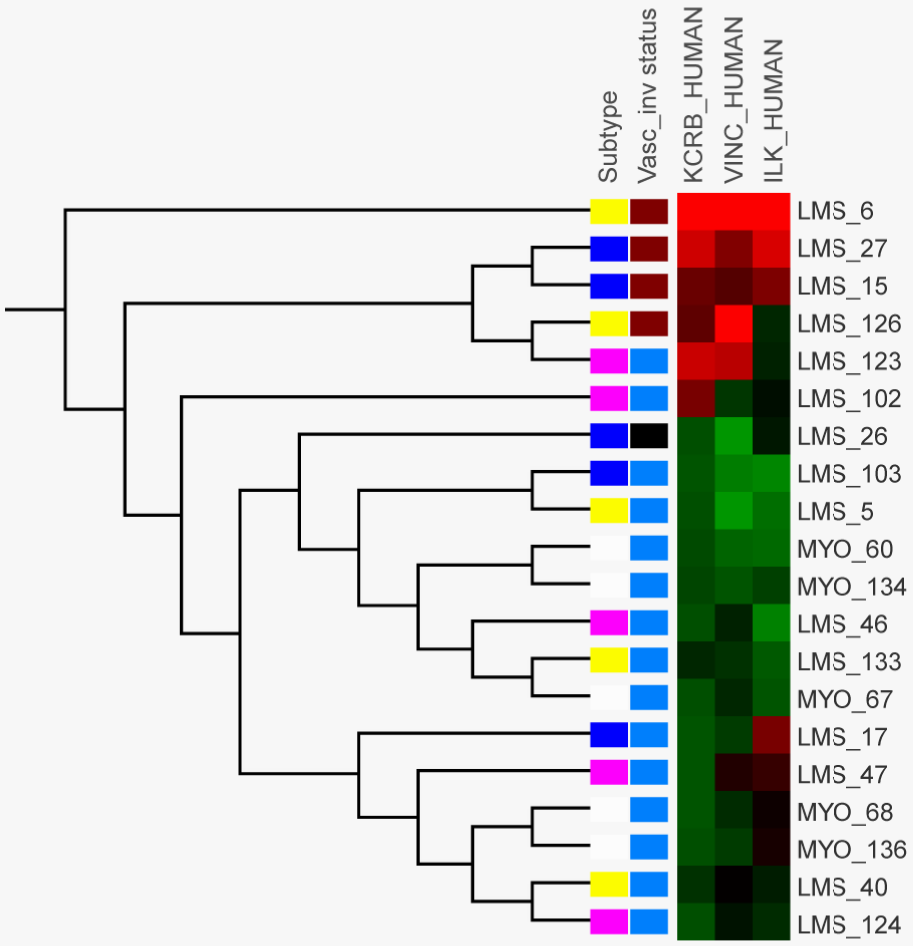

AACR American Association for Cancer Research

Molecular Cancer Research

Discovery-based Protein Expression Profiling Identifies Distinct Subgroups and Pathways in Leiomyosarcomas

Ufuk Kirik, Karin Hansson, Morten Krogh, et al.

Mol Cancer Res Published OnlineFirst July 28, 2014.